# Dense GPS Array as a New Sensor of Seasonal Changes of Surface Loads

Kosuke Heki

*Division of Earth Rotation, National Astronomical Observatory,*
*Mizusawa, Iwate, Japan*

Global Positioning System (GPS) receivers have been deployed worldwide to study inter- and intraplate crustal motions and local deformations associated with earthquakes and volcanic activities. A dense array of GPS is also useful for studying seasonally changing load through periodic components in crustal movements. This article reviews observed and predicted seasonal crustal movements in the Japanese Islands, where both nationwide dense GPS array and meteorological sensor network are available. From comprehensive evaluation of various sources contributing to seasonal signals, the largest factor in Japan is found to be snow, weighing over 1000 kg per square meter in some regions. This is followed by various kinds of loads on the land area, such as atmosphere, soil moisture and water impoundment in reservoirs, and non-tidal ocean loads also cause certain seasonal signatures. Seasonal crustal deformations are calculated by synthesizing all these seasonal load changes, some of which are directly measured meteorologically and others are inferred through models. They are compared with real data observed by the dense GPS array in Japan, and their agreement was examined. The seasonal signals observed by GPS also include artifacts, such as those caused by atmospheric delay gradients and scale changes due to atmospheric refraction. We often discuss subtle crustal deformation signals, e.g. those associated with silent earthquakes, isolating them by removing secular and periodic components. Understanding seasonal signals and their interannual variability is crucial in removing these unwanted signals. The article discusses the Japanese case, but the methods proposed here will be useful worldwide to study seasonal mass redistributions. Dense GPS arrays may play a complementary role to satellite gravity missions in studying seasonal mass redistribution on the Earth in a regional scale.

## 1. INTRODUCTION

Ground stations (receiver and antenna) of Global Positioning System (GPS) are less expensive than other space geodetic techniques like Very Long Baseline Interferometry (VLBI)

and Satellite Laser Ranging (SLR), and suitable for dense deployment near plate boundaries. Relatively small amount of GPS raw data enables data transfer through internet or public telephone line for rapid data analysis in a central station. Crustal deformation data provided by Interferometric Synthetic Aperture Radar (InSAR) are dense in space, but sparse in time because they need almost identical orbits over studied areas. A high sampling rate is possible for GPS, which makes GPS and InSAR complementary techniques. Considering these bene-

fits, a nationwide array of continuous GPS stations, GEONET (GPS Earth Observation Network), has been established in Japan by the Geographical Survey Institute (GSI).

Comprehensive study of global-scale seasonal mass redistribution, including the Earth's response to it, has been done first to explain the observed annual polar motion with geophysical models of mass transports [*Munk and MacDonald*, 1960; *Chao and Au*, 1991]. Recent progress in space geodesy has enabled us to detect such changes in several different ways. Seasonal mass redistribution induces motion of the Earth's center of mass [*Dong et al.*, 1997], which can be estimated by analyzing satellite geodesy data [*Bouille et al.,* 2000; *Crétaux et al.*, 2002]. It also induces deformation of the Earth, which can be measured with worldwide deployed receivers of GPS. *Blewitt et al.* [2001] found seasonal "degree one" deformation (i.e. long-wavelength deformation that can be expressed by the degree one spherical harmonic functions) due to the mass exchange between the northern and southern hemispheres. Higher degree seasonal deformation signals have been detected by *Wu et al.* [2003]. Such mass exchanges can also be observed as the seasonally changing part of the lower order gravity potential coefficients [*Cazenave,* 1999]. Detection of the seasonal changes in higher degree/order gravity coefficients due to mass redistribution is the main target of recent and future satellite gravity missions [*Wahr et al.*, 1998; *Reigber*, 2003].

Comprehensive studies of potential seasonal displacement signal sources were carried out on a global scale by *Dong et al.* [2002]. They evaluated joint contributions of relatively well-known sources, and compared the predicted seasonal coordinate changes with real GPS data to investigate less well-known sources. In order to identify what caused differences between observed and calculated seasonal changes, GPS receivers must be densely deployed, which is not (and probably will not be) the case on a global scale. The Japanese regional network GEONET covers the whole country with inter-site distances of 20–30 km and is ideal for such mass redistribution studies. Seasonal signals have been found in the GEONET GPS site coordinate time series by *Murakami and Miyazaki* [2001]. They investigated their signal structures in detail, but failed to identify the mechanisms responsible for the variation. Later, seasonal signals in northeastern Honshu were interpreted to be largely due to snow loads along the western flanks of the backbone range by *Heki* [2001]. *Hatanaka* [2003a] pointed out the existence of arbitrary seasonal signals irrelevant to crustal deformation in GEONET, namely seasonal scale changes and spurious displacement signals due to atmospheric gradients. Comprehensive evaluation of seasonal loads in Japan is also important to establish a standard method to study seasonal mass redistribution with a dense GPS network in other parts or the world.

Modern satellite geodesy is based on precise determination of satellite orbits. For GPS, this task has been done by the IGS (International GPS Service) for a decade by tracking GPS satellites at fiducial stations whose positions and velocities are given in a terrestrial reference frame. Investigation of seasonal signals is important in assessing the stability of the terrestrial reference frame (and its influence on the errors in the determined orbits) at seasonal time scales. In active plate boundary regions, investigation of seasonal crustal movements is important for crustal deformation studies. *Ozawa et al.* [2002] tried to reveal moment release history of the Tokai slow event, a slow earthquake that started in the middle of 2000. The method they employed to isolate its transient signal is the removal of seasonal and secular components inferred from the time series before the onset of the event. However, such extrapolation is dangerous since it is not guaranteed that these components, especially seasonal changes, behave similarly from year to year. Many such silent events, including silent fault slip after normal earthquakes, are observed in Japan [*Heki et al.,* 1997; *Hirose et al.*, 1999; *Ozawa et al.*, 2003]. Understanding and predicting load-induced crustal deformation would be necessary to extract signals of such events correctly in near real time.

Activities of some kinds of earthquakes in Japan are known to be higher in certain seasons; e.g. interplate thrust events due to the subduction of the Philippine Sea Plate occur mainly in autumn and winter [*Ohtake and Nakahara*, 1999] and inland earthquakes in snowy areas occur more in spring and summer [*Okada*, 1982]. *Heki* [2003] investigated the causal relationship between the snow load and seasonal variation of inland seismicity in Japan by quantitatively estimating disturbances of the Coulomb failure function due to seasonally changing snow loads. He suggested that the removal of snow load associated with the spring thaw may encourage faulting. However, this discussion is based only on the snow load estimated earlier by *Heki* [2001], and lacks evaluation of other kinds of seasonally changing loads. Therefore it is important to evaluate all such loads in terms of their influence upon seismicity.

## 2. SEASONAL CHANGES IN LOADS

The study by *Heki* [2001] had three shortcomings: (1) only the snow was considered as the seasonally changing load, (2) only the northeastern Honshu was studied, and (3) only peak-to-peak amplitudes of the load were discussed. Although it is likely that snow load is the largest seasonally changing load in the northeastern Japan, here I perform a comprehensive study of five different kinds of loads on the entire Japanese islands. This will expand the scope of the study, i.e. the same approach may be applied for other countries where non-snow seasonal loads are important. I also consider the waveforms

of the seasonal load changes to enable better correlation with the observed signals. For these purposes, I divide the Japanese Islands into 130 blocks as large as 0.5° (latitude) and 0.67° (longitude) (Figure 1) and obtain the sum of loads at epochs set up every month (every half month for snow loads) for each kind of loads for each of the blocks. Displacement at each of the GEONET GPS stations by such loads can be calculated in a standard way as the sum of the Green's function describing the elastic response of the Earth to a point load given in *Farrell* [1972].

I did not consider viscous or viscoelastic effects because of the relatively short timescale of the crustal movement discussed in this article. Apart from load-induced displacements, *Hatanaka* [2003a] found that relatively large (and perhaps largely artificial) seasonal scale change of about five parts per billion exists in the GEONET data. I do not try to identify fully the mechanism giving rise to scale changes, but, later in this paper, I model its behavior empirically so that we can remove its contribution from GPS signals. I also exclude discussions on periodic crustal movements whose behaviors are well known and are already corrected in standard GPS data analysis software packages. They include solid earth tide, pole tides (readjustments of the Earth's equatorial bulge to the polar motion), and ocean tidal loading (the Earth's elastic response to ocean tides). Treatments of these corrections in the software package are given in *Hugentobler et al.* [2001], and
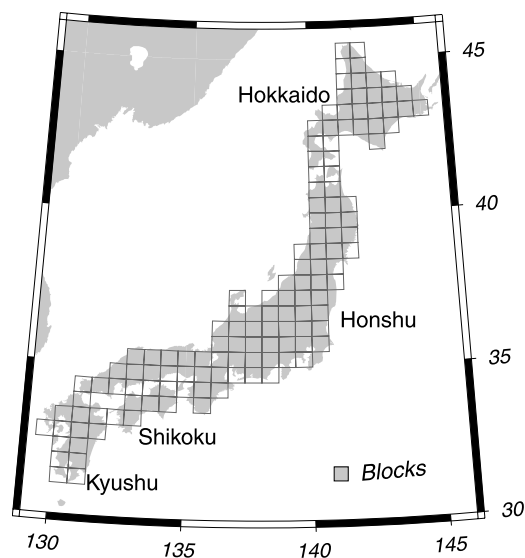


**Figure 1.** The Japanese Islands were approximated with 130 blocks as large as 0.5° in latitude and 0.67° in longitude. Monthly (atmosphere, soil moisture, and dam) or bimonthly (snow) values of loads were obtained for these blocks to calculate elastic response of the Earth (Figures 5–8). Ocean loading was calculated for blocks 1° x 1° in the oceanic area (Figure 9).

those for the GEONET routine analysis are given in *Hatanaka* [2003b].

### 2.1. Snow Load

Snow depth data are obtained daily throughout the snowy area of the country by unmanned snow depth meter as a part of the Automated Meteorological Data Acquisition System (AMeDAS), run by Japan Meteorological Agency (JMA). Figure 2 shows the snow depth curves at three AMeDAS points and averages of the maximum snow depths at AMeDAS stations of the last seven winters. Although the AMeDAS stations are densely deployed, they tend to be located along inhabited valleys rather than in remote mountain areas (they need public electricity and telephone lines). Hence, the elevations of the sites are negatively biased from the national average (the average elevations of snow depth meters is ~200 m, about a half of the Japanese national average). Since snow depths are highly dependent on the elevation in Japan [e.g. *Kazama and Sawamoto*, 1995], this causes serious under estimation of snow depths.

To circumvent this problem, I performed the "altitude correction" for the snow depths by modeling the relationship between the measured snow depths and altitudes of the AMeDAS stations. In Figure 3, I plot snow depths against elevations of the individual AMeDAS sites in different geographical districts. Altitudes of most AMeDAS sites are lower than the district averages. For such districts, I basically used prefectures (about fifty in total) since they correspond to areas with relatively uniform meteorological setting surrounded by natural boundaries such as mountain ranges and seashore (from this viewpoint, blocks shown in Figure 1 are not suitable for this purpose). Average altitudes of Japanese prefectures are available at http://iide.hp.infoseek.co.jp/zatu/zatu6.htm. Some small neighboring prefectures with similar climates were amalgamated as one large district (e.g. Toyama Pref. and Ishikawa Pref.) while large prefectures composed of snowy highlands and snow-free lowlands were commonly divided into two districts (e.g. Fukushima Pref.).

Within such a district, snow depths increase approximately linearly with altitudes suggesting that the altitude is the main factor to control the amount of snow on a local scale. Slopes are slightly different between districts reflecting different geographical and meteorological settings. In this study, I performed linear regression for each district, and then the altitude correction for every AMeDAS site was obtained by multiplying the slope and the difference in altitudes between the AMeDAS site and the prefectural average. This correction was added to the raw AMeDAS snow depth value to make it more realistic. Then the daily snow depth data at the AMeDAS
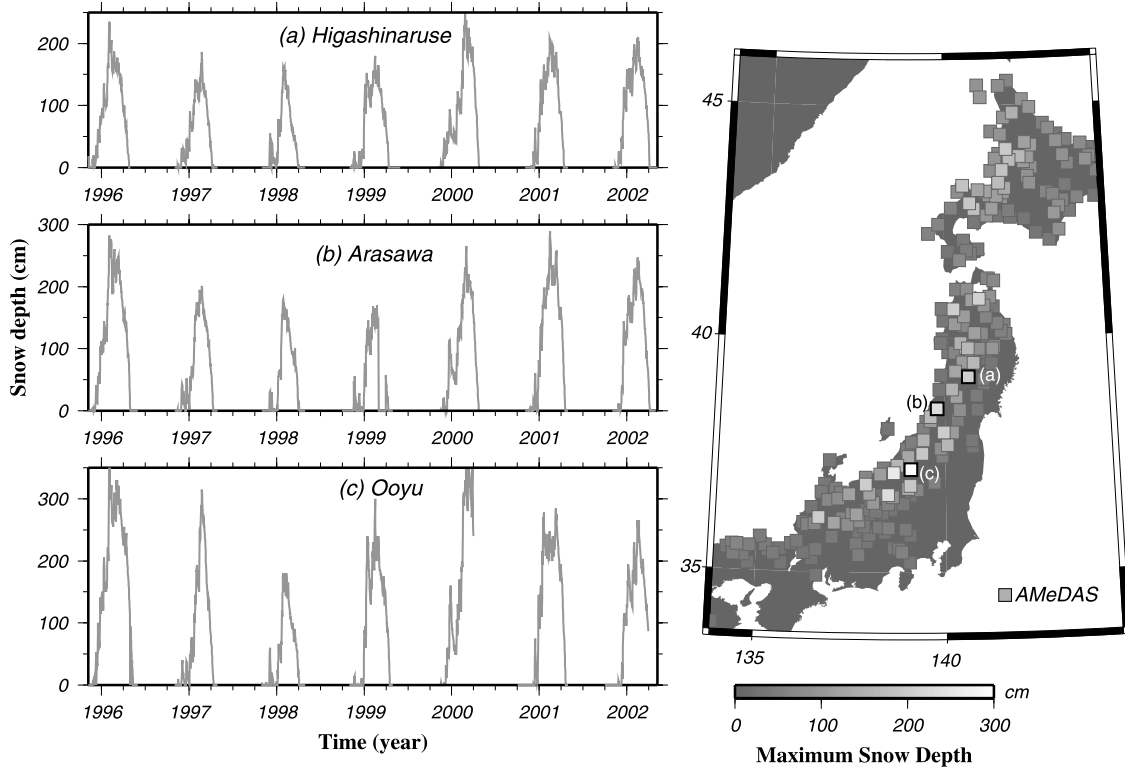
**Figure 2.** Daily snow depth measurements at three AMeDAS sites, (a) Higashinaruse (Akita Pref.), (b) Arasawa (Yamagata Pref.) and (c) Ooyu (Niigata Pref.), indicated as squares with bold frames in the map, from north to south, over the seven winter seasons 1996–2002 (left graphs), and distribution of the average of the maximum snow depths of the seven winters at the AMeDAS sites equipped with snow depth meters (right map).

sites after district-wise altitude corrections were compiled to calculate block-wise bimonthly average snow depths. Scatter in Figure 3 reflect within-district differences of factors controlling snow, e.g. orientation of topography relative to
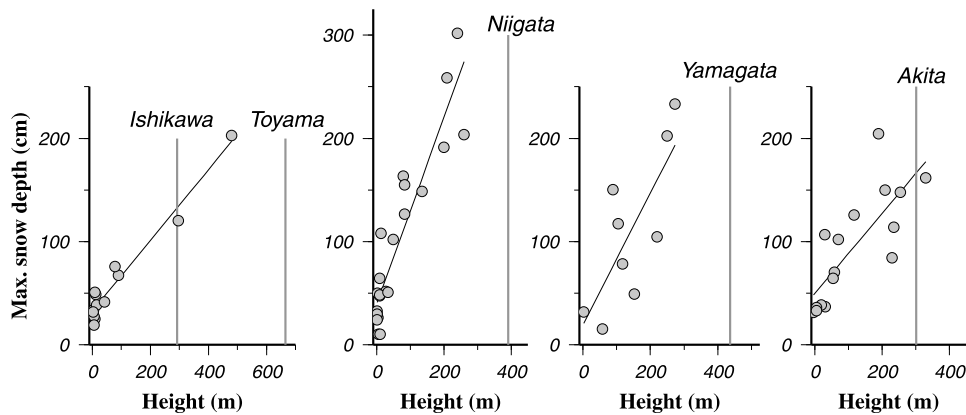


**Figure 3.** Relationship between the average maximum snow depths (same as Figure 2 right) and elevations of the AMeDAS snow depth meter sites (best-fit lines are shown in black). They were plotted for snowy prefectures along the Japan Sea coast of Honshu (Akita, Yamagata, Niigata, Toyama and Ishikawa Prefectures, from northeast to southwest). Ishikawa and Toyama are plotted together in one diagram. Vertical gray lines show average elevation for these prefectures, and dots denote AMeDAS stations. Most AMeDAS sites are located below average altitudes, and realistic snow depths of the entire prefectures have to be inferred considering their altitude dependence.
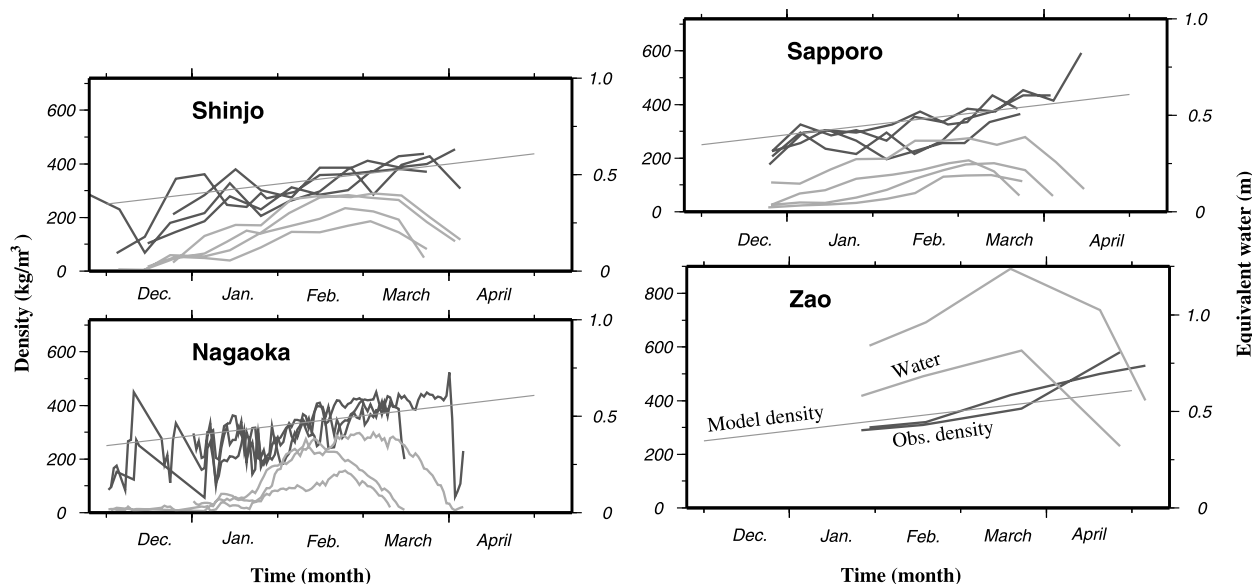
**Figure 4.** Light and dark gray lines indicate the time series of the total amount of snow in terms of equivalent water depth (scale to the right) and average density of snow (scale to the left) over winter months. The data were taken at four sites, namely Sapporo (Hokkaido), Zao (Miyagi-Yamagata Pref. boundary), Shinjo (Yamagata Pref.) and Nagaoka (Niigata Pref.). Years when the data were obtained are different between the sites. It is shown that snow mass is the largest in late February or early March, and snow density increases monotonously with time. Model density shown by gray straight lines is assumed as the common standard.

main weather systems, overall size of mountain region and local topographic effects. This makes the uncertainties of the corrected snow depths 10–30% of the estimated values depending on the amount of scatter.

To convert snow depths to loads, we need the average density of the snow cover, which generally increases toward the end of winter due to compaction. *Heki* [2001] adopted 400 $kg/m^3$ as the instantaneous snow density at the time when snow loads are the largest (assumed as middle of March), but here I need its continuous temporal change from December to May to model bimonthly loads. I compiled snow density data collected at four points in Japan (Figure 4), namely Sapporo (snow cross section data were available annually from the Low Temperature Res. Inst., Hokkaido Univ., Sapporo, Hokkaido, e.g. *Hachikubo et al.* [1997]), Shinjo (Yamagata Pref.), Nagaoka (Niigata Pref.) (both observatories are run by Nat. Inst. Disaster Prevention and Earth Sci., and data are available at http://romalia.bosai.go.jp/seppyo/), and the top of Mt. Zao (boundary between Yamagata and Miyagi Prefs.) [*Yamaya et al., 1999*].

Despite the difference in winter temperatures and altitudes, the average density values at these points are fairly uniform, starting with ~200 $kg/m^3$ and reaching ~400 $kg/m^3$ when the snows are deepest. In this study, I use the unified model of the snow density; it starts with 250 $kg/m^3$ at the beginning of December, increasing with time by ~40 $kg/m^3$/month, attain-

ing 400 $kg/m^3$ at the end of March. This model is shown as a line in each panel of Figure 4. By multiplying the snow depth by such time-dependent density, I obtained bimonthly block-wise snow loads. Figure 4 shows that the observed snow densities scatter around the model by a few tens of $kg/m^3$, which will cause additional error of ~10% to the estimated snow loads. Figure 5 shows differences between the maximum and minimum (zero in this case) snow loads for the blocks. Large snow loads are distributed along the northwestern flanks of the backbone range, while they are almost absent along the Pacific coast and in the southwestern Japan. As shown in the insets of Figure 5, snow loads are characterize by strong peak in winter and a relatively flat period during the rest of the year.

### 2.2. Atmospheric Loads

Changes in atmospheric pressure and the corresponding displacements of space geodetic stations have been studied for many years [*van Dam et al.*, 1994]. Response of the solid earth to the atmospheric load obeys the same theory as the snow. Atmospheric load, unlike snow, acts both on the land and ocean. However, relatively long period (e.g. annual frequency) pressure changes do not exert on the sea floor since they are effectively compensated by natural adjustment of sea surface height (inverted barometer hypothesis). The coefficient to convert pressure changes to displacements hence
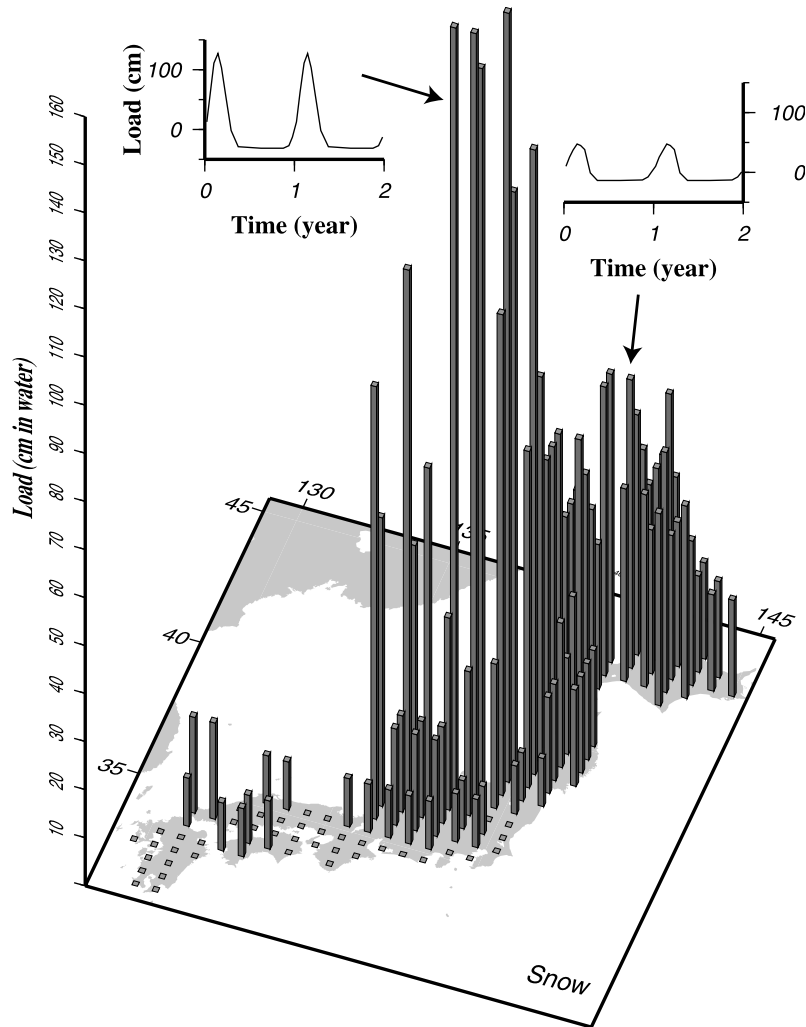
**Figure 5.** Difference between the maximum and the minimum (zero in this case) value of snow load for blocks shown in Figure 1, obtained from the last seven winters of AMeDAS data converted to those at prefectural average elevations. Insets are time series of seasonal load changes at the two selected blocks indicated by arrows. Since the annual averages are adjusted to zero in these inset graphs, loads take small negative values during summer.

depends on the shoreline geometry around the site. In this study I assume that atmospheric load works only on the land area. I model monthly mean pressures for individual blocks (Figure 1), using average meteorological data over the last few years at 80 sites available in *Naional Astronomical Observatory* [2002]. Pressure values in blocks without data points were interpolated using values of neighboring blocks. I did not use AMeDAS data because of smaller spatial variation of the pressure than snow. In general, pressure tends to be high in winter and low in summer in Japan, and the seasonal change has a complicated waveform in northeastern Japan (Figure 6 inset). Amplitudes of seasonal variation are larger in western Japan, where the peak-to-peak changes amount to 1.5 kPa (~15 cm water column). They are less than 1 kPa

in northeastern Japan. Figure 6 shows distribution of peak-to-peak atmospheric load changes.

Short-term intra-seasonal pressure variations often exceed annual variations in amplitudes. For example, the 21st typhoon of 2002 hit the Kanto Area on 1st October, and brought several kPa pressure dip lasting for a few hours. Crustal strain changes caused by such transient removal of atmospheric load were observed by borehole-type three-component strainmeter [*NIED,* 2003], but the signature was not obvious in coordinate time series of GPS stations made of daily averages. It would be an interesting future issue to investigate, by kinematic positioning technique, how far the inverted barometer hypothesis remains valid for such short-term disturbances.
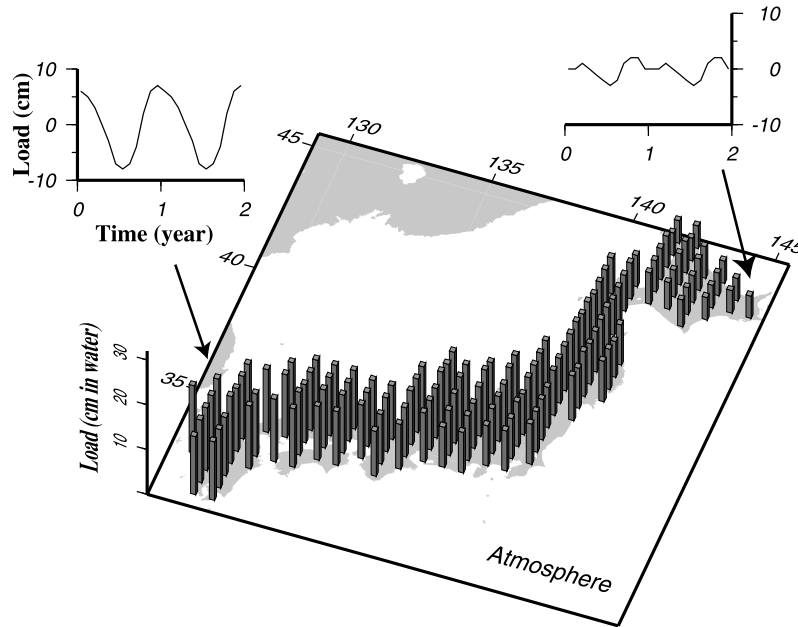
**Figure 6.** Peak-to-peak amplitudes of seasonal atmospheric pressure changes at the blocks, with two insets showing variations at two selected blocks.

### 2.3. Soil Moisture

Seasonal variation of continental water storage, including snowpack, soil moisture, and groundwater, causes mm to cm level vertical crustal movements [*van Dam et al.,* 2001]. Here I model the soil moisture changes in individual blocks (Figure 1), with a simple model constructed using the following three quantities, i.e., (1) potential evapotranspiration (PET), (2) precipitation, (3) water-holding capacity in soil. Following a simple model by *Milly* [1994], soil water is assumed to increase by precipitation and decrease by evapotranspiration. When the water exceeds the storage capacity of soil, the excess amount runs off keeping soil water at its maximum level. When the PET is larger than the available soil water, all soil water is lost due to evapotranspiration and the water level becomes zero.

Such calculations were performed at 80 points where meteorological data are available with monthly time steps. The monthly PET was calculated as a function of temperature and length of daytime following the formula given in *Thornthwaite* [1948]. Monthly mean temperature and precipitation were taken from *National Astronomical Observatory* [2002]. Here I did not use the AMeDAS data, either, considering rather smooth spatial variation of the meteorological data. Water storage capacity depends on the type and thickness of the soil, and is basically unknown. Precipitation exceeds PET almost all time in most places in Japan, and the soil water level is maintained at levels close to the water storage capac-

ity. Thus, unless the storage capacity is unrealistically small, the soil water never runs out and we could calculate seasonal soil water changes without information on the capacity.

Simulation of monthly soil moisture values for individual blocks showed that the load changes are smaller than those related to the atmosphere in most regions (Figure 7). The largest variation occurs in the inland area of the southwestern Japan and Hokkaido, where summer precipitation falls below PET and soil water levels temporarily become lower than maxima for a few months. In cold regions, input of solid precipitation (e.g. snow) into soil could delay until the spring thaw. Such a delay is neglected in this study since it causes delay in runoff rather than in soil moisture change, because soils are nearly saturated with water during winter and spring. Change in groundwater (water in aquifer below soil layer) may locally cause vertical crustal movements in Japan [*Munekane et al.*, 2003], but this was not modeled in this study because its seasonal change is not well known. Impoundments during summer months of rice fields (usually as deep as ten centimeters or so), which occupy about ten percent of the land, are not considered, either. Its influence would not exceed those considered in this article.

### 2.4. Water Impoundment in Reservoirs

Water mass reserved in increasing number of reservoirs is large enough to change the low degree gravity coefficients [*Chao*, 1995]. Impoundment of several largest dams, e.g. the
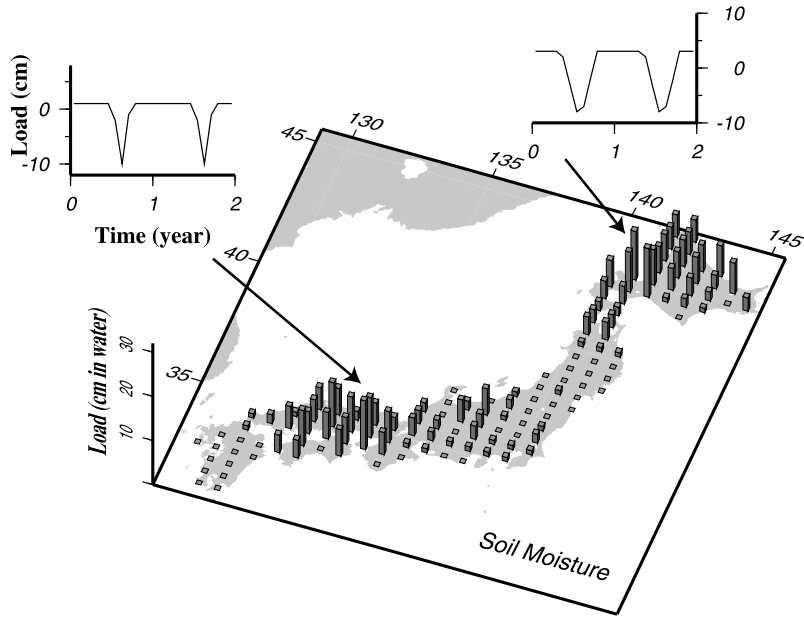
**Figure 7.** Peak-to-peak amplitudes of seasonal soil moisture load changes at the blocks.

Three Gorges Dam, China, causes crustal deformation large enough to be detected by space geodesy [*Wang et al.*, 2002]. Japanese dams are smaller; even the largest one (the Okutadami dam, Fukushima Pref.) has the capacity of only 600 million tons, two orders of magnitudes smaller than the world largest dams. However, dams are densely distributed in Japan, and their total water storage may be worth considering. I compiled water capacities, coordinates of 546 dams with capacities larger

than five million tons (information available from the Japan Dam Foundation, http://wwwsoc.nii.ac.jp/jdf/Dambinran/binran/TopIndex.html).

Pattern of seasonal change of water level varies from dam to dam as well as from year to year. Roughly speaking, there are two types of patterns, i.e. those of reservoirs in snowy areas and in snow-free areas. The latter is characterized by one peak, i.e. high water level in winter and low level in summer (Figure
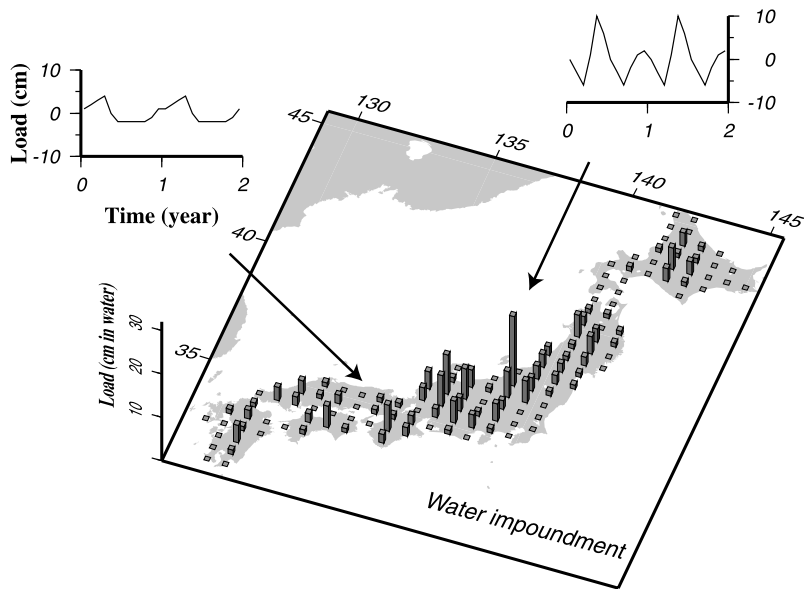


**Figure 8.** Peak-to-peak amplitudes of seasonal load changes by water impoundment of reservoirs at the blocks.
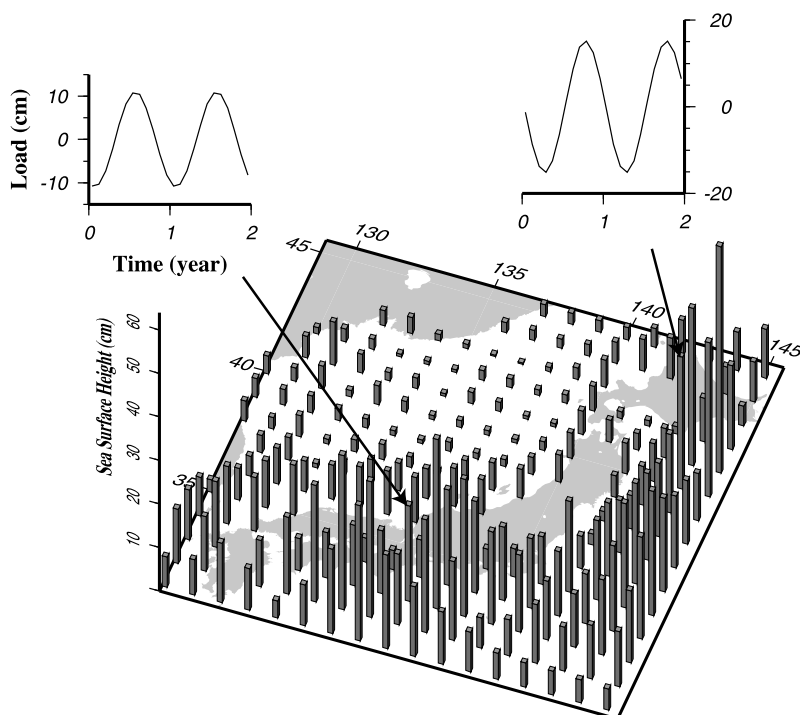
**Figure 9.** Peak-to-peak amplitudes of seasonal ocean load changes at the 1° x 1° blocks in the oceanic area around Japan, with two insets showing variations at two selected blocks.

8 left inset). The former shows more complicated patterns. Water levels decrease during snow-covered period, and increase in spring thaw attaining the first peak of a year. Then, they fall again in summer and rise during autumn toward the second peak around the onset of snowy season (Figure 8 right inset). I adopted the 9 years average seasonal water level change curve of the reservoirs in the Kanto District available in http://www.ktr.mlit.go.jp/kyoku/1_topics/16_mzshi/mizu_02.htm. The peak-to-peak amplitude of water level variation of a reservoir was adjusted to a half of its total capacity. I classified Japanese reservoirs into the two types, and calculated monthly sums of the water loads at these reservoirs for individual blocks. As seen in Figure 8, the variation is large in some mountainous blocks in central Japan, often exceeding 10 cm in within-block averages. However, they are much less than the two major contributors, i.e., snow and atmosphere.

*2.5. Ocean Loading*

Tidal ocean loading causes half-daily crustal movement above the detection level of GEONET [*Hatanaka et al.*, 2001] but is corrected in the GEONET solutions [*Hatanaka*, 2003b]. Sea surface heights (SSH) change seasonally such that the sea surface in September is higher than in March by 20 cm or more [*Okada*, 1982; *Kato*, 1983]. This includes

thermal expansion irrelevant to load changes, which must be removed to consider seasonal changes of pressure at the ocean bottom. Annual changes in gravity are considered to be the sum of the contributions of polar motion, solid earth tide, and the effect of sea water mass changes [*Sato et al.*, 2001]. They corrected the SSH seasonal variation in the Parallel Ocean Climate Model (POCM) [*Stammer et al.,* 1996] for thermal expansion assuming various thermal steric coefficients. The observed annual gravity changes best coincide with predictions when the coefficient is 6.0 mm/degree. They removed thermal expansion contribution using this coefficient and the seasonal variation of sea surface temperature in POCM, and found residual annual variation of SSH with amplitudes exceeding 10 cm around Japan (Figure 3 of *Sato et al.,* [2001]). Peak-to-peak seasonal variations of sea water mass at the 1° x 1° squares around Japan show a large increase in ocean loads in the Pacific Ocean in summer while they are almost stationary throughout a year in the Japan Sea (Figure 9). This gives rise to seasonal translation of the whole Japanese Islands by about 1 mm, but crustal deformation within Japan does not exceed those by soil moisture and water impoundment in reservoirs. Ocean loading models still have large uncertainties and we would need their further refinement, e.g. by satellite measurements of seasonal gravity changes [*Wahr et al.*, 1998] and by
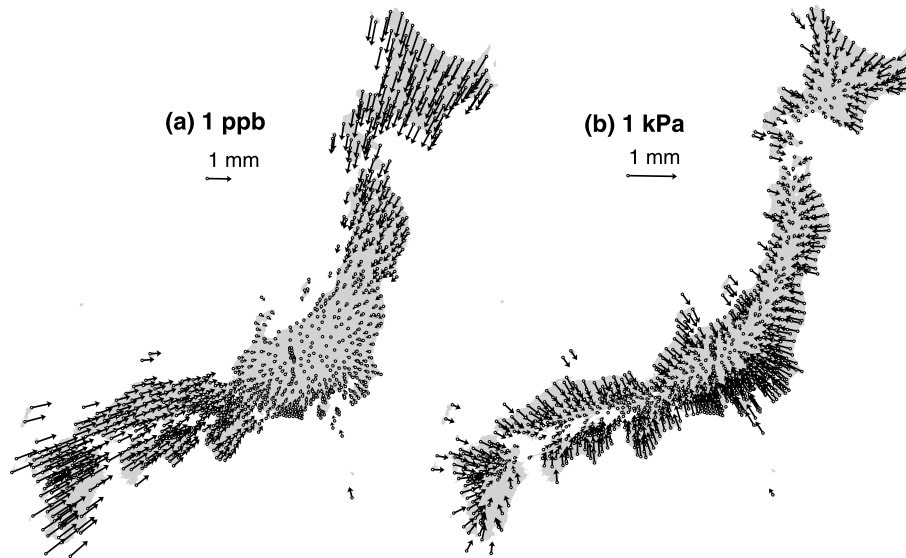
**Figure 10.** Comparison of seasonal coordinate changes due to isotropic scale change (1 ppb contraction) (a), and load (1 kPa uniform load on land area) (b). They are characterized by arc-parallel and arc-normal contraction, respectively, and can be easily discriminated.

deploying ocean bottom pressure gauges [*Fujimoto et al.*, 2003].

## 3. SYNTHESIS

### 3.1. Seasonal Scale Change

Geodetic positioning often suffers from the scale problem, namely an ambiguity in uniform expansion or contraction of the whole network. It is typically seen in classical triangulation surveys; measured length of a certain baseline determines the scale of the whole network. Even in space geodesy, the scale is controlled by several quantities, e.g. the speed of light, the Earth's GM (product of the universal gravity constant and the Earth's mass), error in GPS center-of-mass to antenna phase-center offsets, and many other factors [*Beutler et al.*, 1988]. In most cases, such scale changes are considered to be artifacts irrelevant to real crustal deformation, and scales have been readjusted in combining positioning results obtained with different techniques to establish global terrestrial reference frames [e.g. *Altamimi et al*, 2002].

In Japan, *Hatanaka* [2003a] found that the whole GPS network repeats annual cycles of uniform expansion in summer and contraction in winter (seasonal scale change) of about 5–6 part per billion (ppb) in addition to real crustal deformation due to seasonally changing loads. Isotropic contraction causes substantial shortening of arc-parallel baselines as shown in Figure 10a. Because Japan is an island arc elongated in northeast–southwest, load uniformly distributed over land

mainly gives rise to arc-normal contraction (Figure 10b). In order that surface loads cause such a uniform contraction, there should be an equal amount of seasonal changes of loads over the land and seafloor. This is quite unlikely. The seasonal degree one deformation [*Blewitt et al,* 2001] causes almost uniform regional expansion (contraction) in summer (winter), but this is no more than 1 ppb in Japan. Therefore substantial part of the 5–6 ppb scale change in GEONET would not be seasonal deformation of the real Earth, but an artifact.

GEONET site coordinates are estimated using the Tsukuba station, Ibaraki, as the fixed reference. *Munekane et al.* [2003] reported that this station repeats seasonal vertical movement with peak-to-peak amplitude of ~2 cm due to extraction of groundwater for agricultural purposes in spring. *Beutler et al.* [1988] suggests that such a vertical coordinate error of the fixed site causes a ~0.6 ppb seasonal scale change (contraction in winter). This effect, together with the seasonal degree one deformation [*Blewitt et al,* 2001], accounts for ~20% of the observed scale changes. In addition the pole tide could give rise to annual and Chandler period height change with amplitude of ~1 cm. However, it does not cause scale changes because they are corrected beforehand in the GEONET solution [*Hatanaka,* 2003b], following the IERS standards [*McCarthy,* 1996]. *Beutler et al.* [1988] also suggests that an error in absolute atmospheric delay causes scale changes. *Hatanaka* [2003a] considered that this possibly causes the unexplained part of the scale change. He plotted the difference between wet atmospheric zenith delay obtained by GPS and by water vapor profile obtained by radiosonde, and
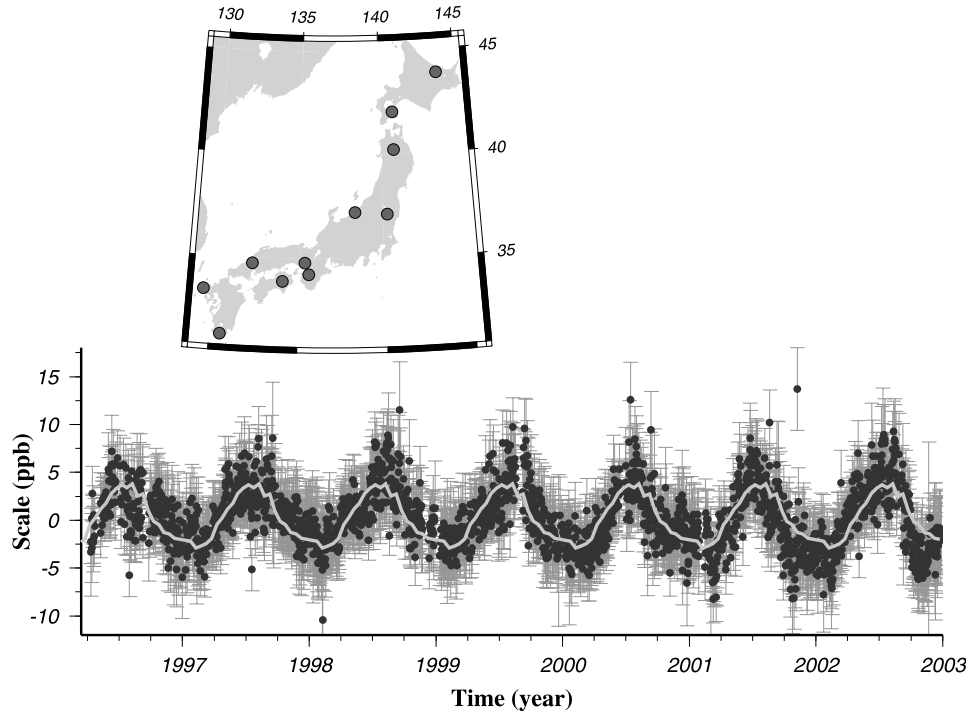
**Figure 11.** Daily scale values were estimated using time series of site coordinates at ten sites in the inset map after removing secular trends. Average seasonal scale variation composed of bimonthly values (thick gray curve) was estimated by stacking these scale changes over seven years.

found that the seasonal changes in the differences are almost consistent with the observed scale changes. However, there is no a-priori reason to consider only the GPS-based water vapor data wrong, and it is premature to conclude that the scale problem is solved.

In the present study, instead of trying to clarify the mechanisms for the scale change, I apply an empirical model according to the following procedure. I take out ten stations which are well distributed over the country and free from transient signatures related to recent seismic or volcanic activities. I remove secular components from their daily coordinate time series. Then the residual coordinate time series 1996–2003 are used to estimate daily values of scales (Figure 11). Seasonal behavior of scale is fairly uniform year after year, and from them I obtained the average seasonal changes composed of bi-monthly scale values. This is possible because the scale change signature is very "different" from load signature as shown in Figure 10. Such a "difference" comes from the elongated shape of the Japanese Islands, and so the discrimination between scale and load signatures could be difficult in other countries.

In addition to seasonal scale changes, *Hatanaka* [2003a] pointed out atmospheric delay gradients [*MacMillan*, 1995; *Miyazaki et al.*, 2003] are significant in the north–south direction at stations along the Pacific coast of the central and southwestern Japan. They cause apparent northward movement of southern stations in winter relative to the Japan Sea side of the arc. This contributes to arc-normal contraction in southwestern Japan in winter, and enhances signals of seasonally changing loads. By repeating data analyses with and without estimation of atmospheric gradient parameters, *Hatanaka* [2003a] found that this contribution may amount up to a few mm. Because GSI does not estimate atmospheric gradients in their official GEONET solution at the moment [*Hatanaka*, 2003b], the current solution includes apparent seasonal crustal movement due to this effect.

### 3.2. Sum of Contributions

In Figure 12, I show the sum of the displacements of GPS sites in winter relative to summer of the five seasonal loads considered in this study (Figures 5–9). In this figure, a station on the Japan Sea coast (the Oogata station) is held fixed. Arc-normal contraction in winter of up to 4–5 mm is seen in the northeastern Japan. Since the fixed station subsides in winter due to snow load, GPS sites in snow-free southwestern Japan apparently go up in winter. These features are consistent with the basic pattern of seasonal crustal deformation in northeastern Honshu discussed in *Heki* [2001] although he considered only snow loads. Snow-induced signals are thus
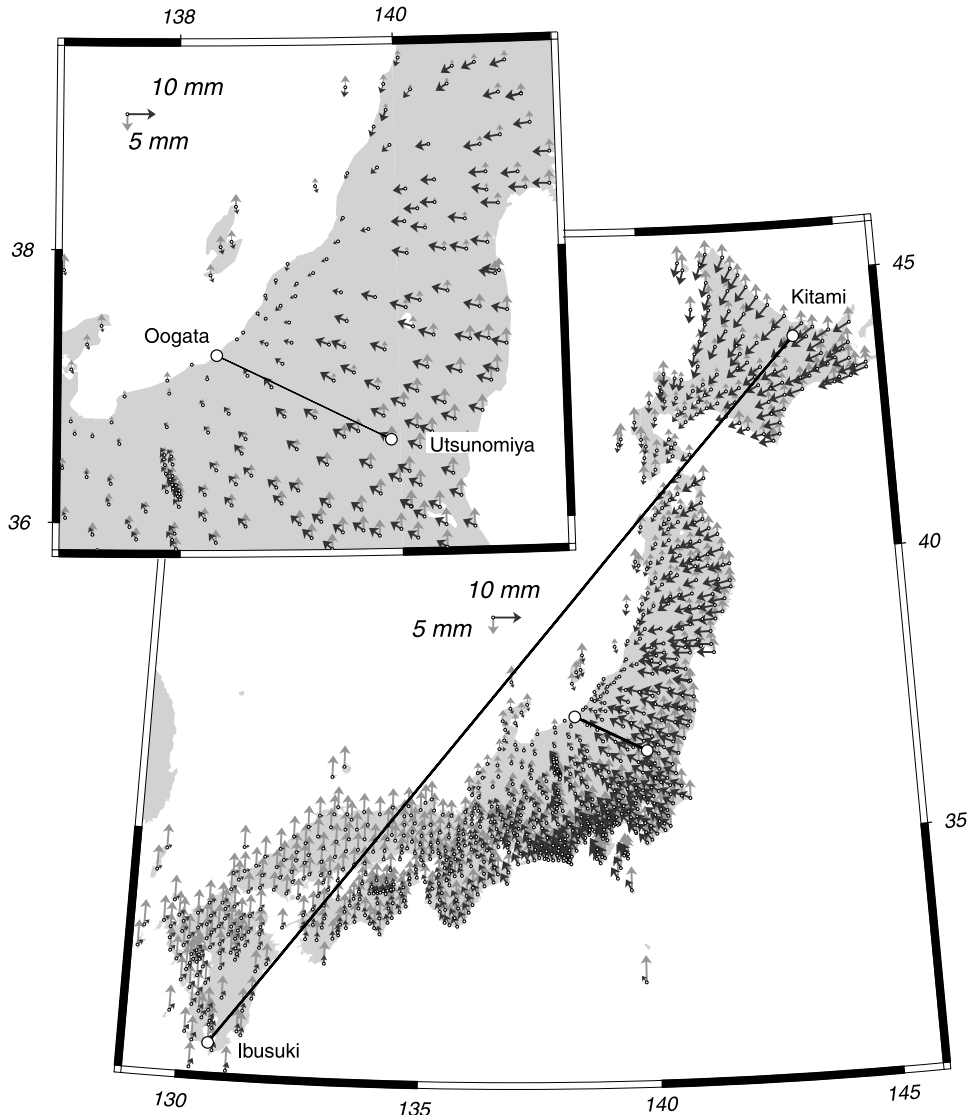
**Figure 12.** Seasonal displacement (early February position with respect to the early August position) due to joint contribution of snow, atmosphere, soil moisture, water impoundment in dam and ocean loads. The Oogata station is held fixed. Contributions from individual sources are compared in Figure 13 for lengths of the two baselines shown in the map.

predominant as long as relatively small regions (up to a few hundreds of kilometers level) in the northeastern Japan are concerned. Actual GPS data include components coming from the seasonal scale changes, whose contribution becomes predominant as the studied area expands.

Examples showing relative importance of various kinds of loads and scale are shown in Figure 13. Contribution of scale change simply depends on baseline lengths; those longer than 1000 km vary by 5–6 mm by seasonal scale changes, which is larger than any real load signals. For example, major source of seasonal changes for a long baseline connecting Hokkaido and Kyushu (Figure 13a) is the scale change, with additional

contributions of snow, ocean loading and atmosphere. In a relatively short baseline in central Japan (Figure 13b) contribution of snow is the largest, being followed by scale change and atmosphere. Contribution of snow loads is characterized by sharp negative peaks in winter and relatively flat period lasting from spring to autumn. Other components, mainly scale and atmospheric load, bring broad positive peak in summer making the total waveform more like a sine curve.

Soil moisture, water impoundment in reservoirs, and non-tidal ocean loading were relatively minor in Japan, but these factors could be major contributors in other parts of the world. For example, in relatively dry areas with precipitations con-
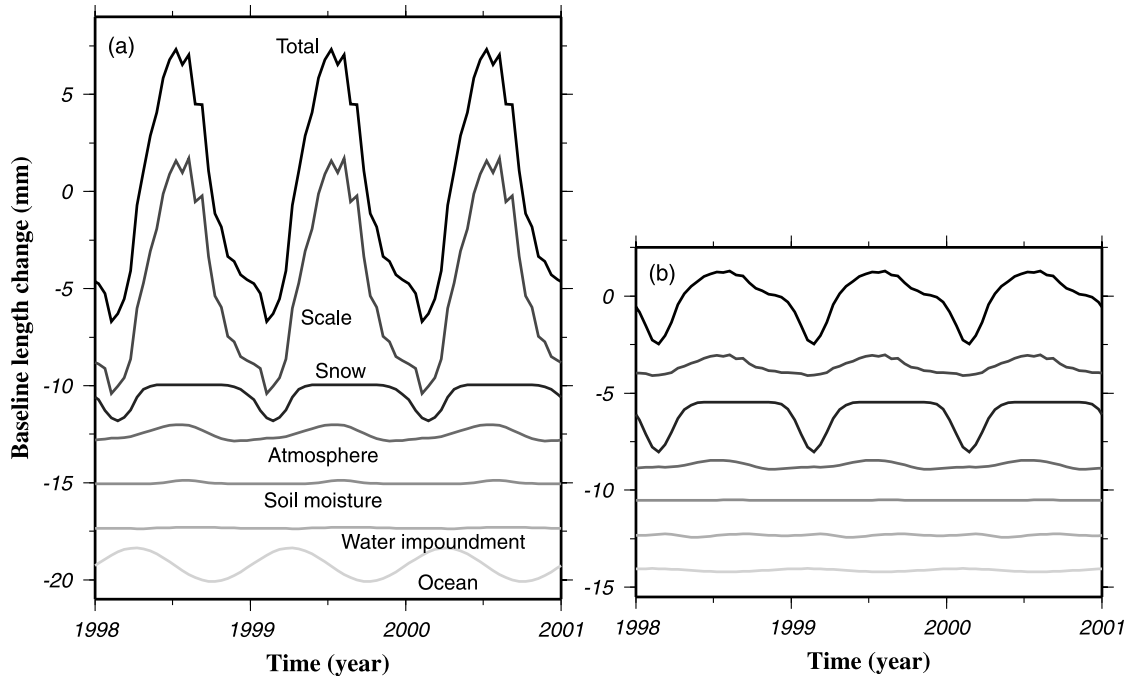
**Figure 13.** Seasonal change in lengths for two baselines shown in Figure 12, Kitami-Ibusuki (a) and Oogata-Utsunomiya (b). Contributions from scale, snow, atmosphere, soil moisture, water impoundment and ocean are shown from top to bottom.

centrating on a certain time of the year, soil moisture may change by several tens of centimeters as a equivalent water column. In an oceanic island, seasonal changes in ocean circulation could cause significant displacement of the island. In this article I have tried to explain the observed seasonal signals in Japan. However, the same approach to study seasonally changing loads could be used in other parts of the world if there are networks of geophysical (meteorological) sensors with quality and density similar to the present case.

### 3.3. Comparison With GPS Observations

Here I compare synthesized seasonal signals with those observed by GEONET. I employ the newest solution based on the improved analysis strategy [*Hatanaka*, 2003b]. Figure 14 compares seasonal signals in the lengths of five arc-normal baselines. They are relatively short, and real crustal deformation signals are predominant like in Figure 13b. Several features seen in Figure 13b, e.g. strong negative peak in winter and broad positive peak in summer, are reproduced to some extent in Figure 14. The southernmost baseline (baseline E, Figure 14) show somewhat larger seasonal variations than predicted. Part of such difference may be an artifact coming from the north–south atmospheric gradient of the southern station as discussed in section 3-1. Arc-parallel baselines are shown in Figure 15. They are longer and are more affected

by scale changes than those in Figure 14, although snow load has significant contributions in northern Japan. The observed seasonal signals are also fairly consistent with predicted curves; northern baselines have sharper winter peaks reflecting the snow signature, and such peaks get broader toward the south reflecting the dominance of the scale change.

Such features are confirmed by the behavior of the root-mean-squares (rms) for various cases shown to the right of Figures 14 and 15. There I show the two extremes, i.e. rms for the case of best-fit seasonal (annual plus semiannual) change curves (black column), and rms for the case without seasonal signals (rightmost gray column). Cases with a-priori seasonal curves considering all or part of the six contributors (scale, snow, atmosphere, soil moisture, water impoundment in reservoirs, and ocean loads) are shown between these two extremes. In spite of the large uncertainties in the snow load as explained in section 2-1, the a-priori corrections give almost as small rms as the a-posteriori best-fit seasonal changes, suggesting that the current approach has been acceptable.

While baseline length changes in Figures 14 and 15 mainly reflect horizontal coordinates and include significant amount of scale change contributions, vertical components are less affected by scale changes and respond mainly to loads. Figure 16 shows seasonal vertical movements at four sites in snow covered area and one in snow-free area, relative to a fixed station in a snow-free area. Although the signals are
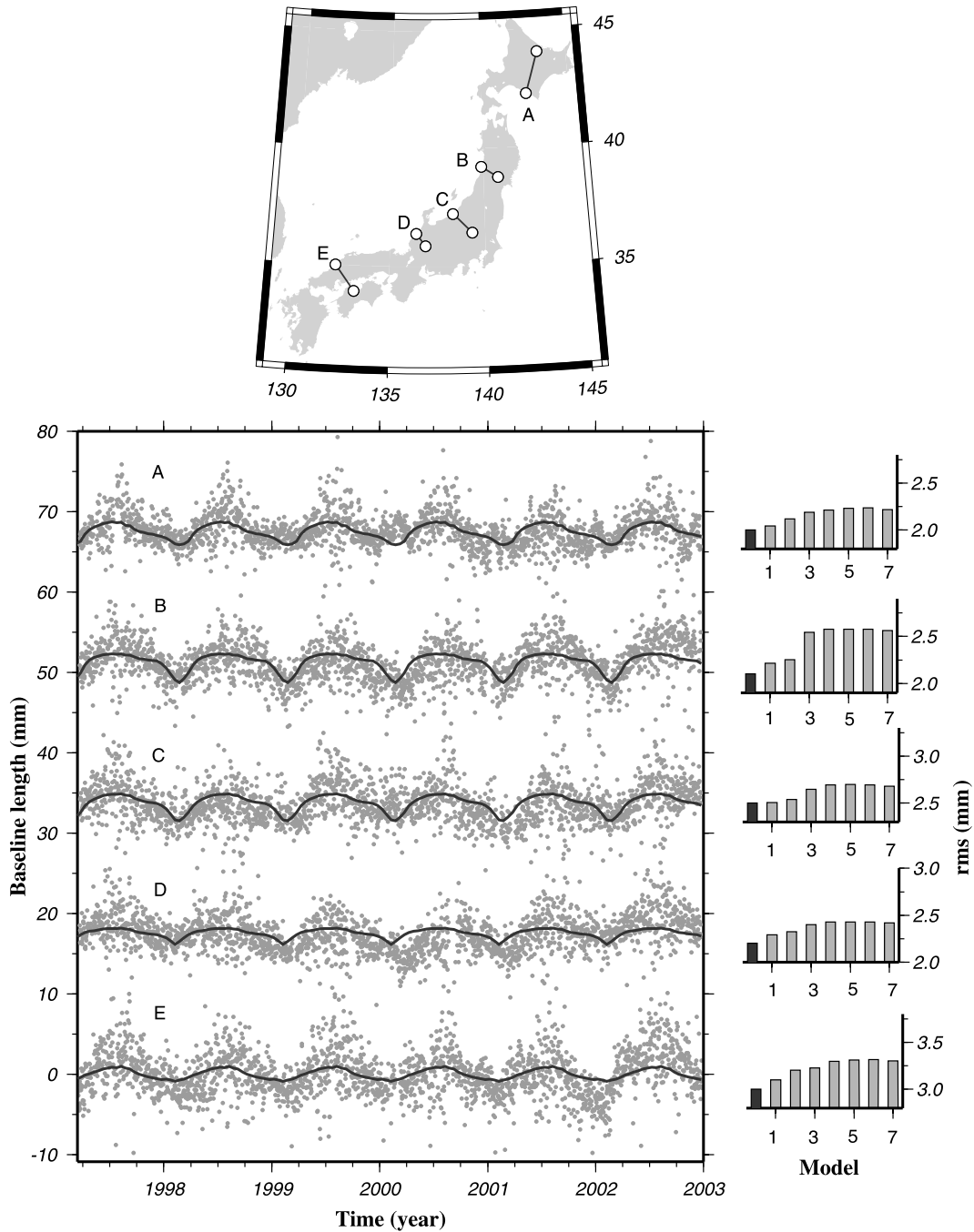
**Figure 14.** Seasonal change in lengths for five arc-normal baselines shown in the map at the top. Dots are daily solution of GPS (secular trends are removed beforehand) while curves denote seasonal variation curves synthesized in a similar manner to Figure 13. Diagrams indicated to the right for individual baseline data show root-mean-square (rms) of the differences between the GPS data and the synthesized model values. The black column to the left denotes rms values obtained a-posteriori by estimating best-fit seasonal (annual plus semiannual) curves for the GPS data. Gray columns (model number 1 to 7) are rms values obtained a-priori by assuming (1) all of the seven contributors, (2) without scale, (3) without scale and snow, (4) without scale, snow and atmosphere, (5) without scale, snow, atmosphere and soil moisture (i.e. only water impoundment and ocean), (6) without scale, snow, atmosphere, soil moisture, and water impoundment (i.e. only ocean), (7) without scale, snow, atmosphere, soil moisture, water impoundment and ocean (i.e. no seasonal variation).
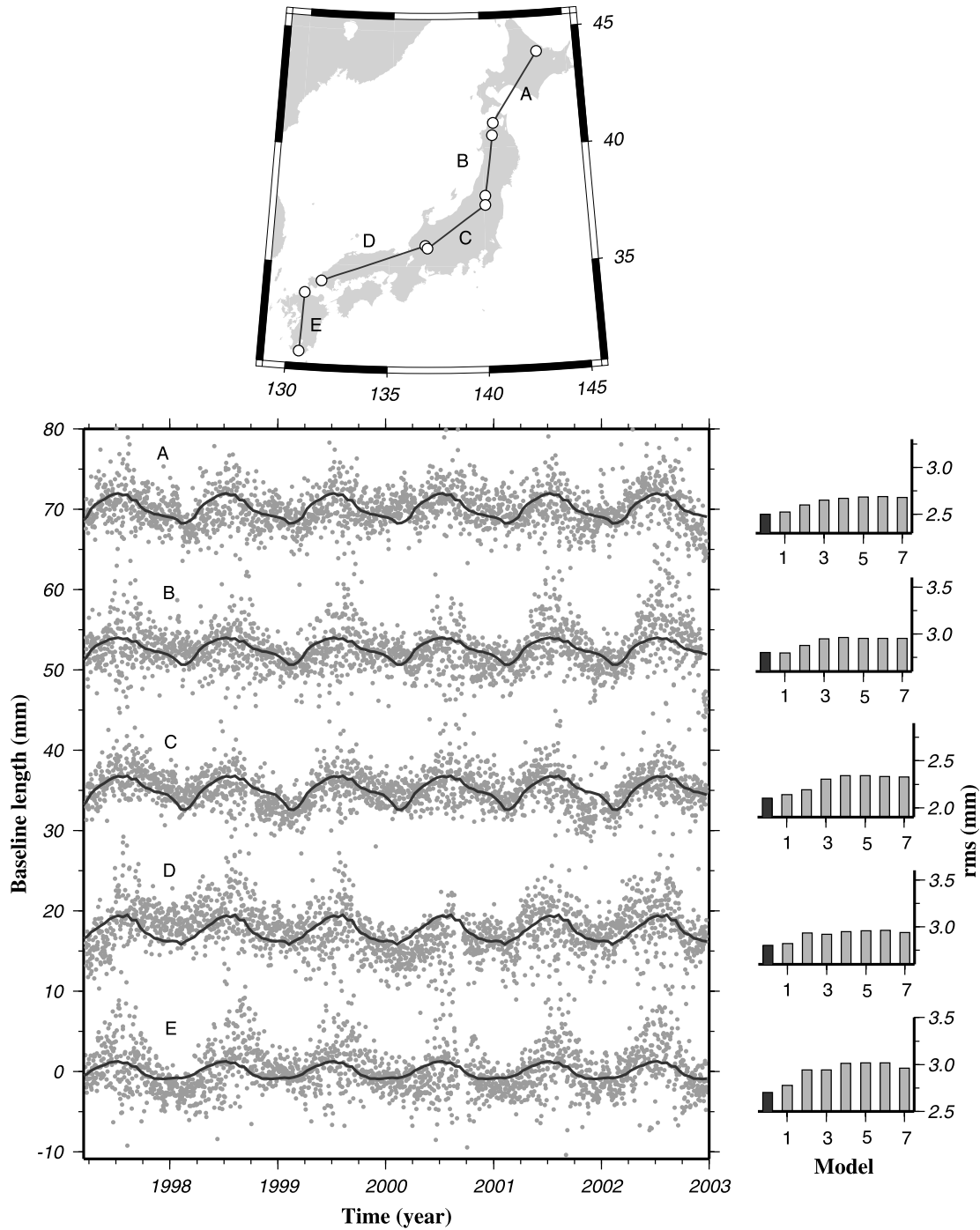
**Figure 15.** Seasonal change in lengths for five arc-parallel baselines shown in the map at the top. See the caption of Figure 14 for detail.

noisier than the baseline lengths shown in Figures 14 and 15, winter subsidence of about 1 cm can be seen at snow-covered stations. We also notice unexpected strong summer peaks in observed signals, which makes the amplitudes larger than predicted. Such tendency is not clear in horizontal components as seen in Figures 14 and 15, and is possibly of atmospheric origin. Relative atmospheric delay errors tend to give rise to height errors [*Beutler et al.*, 1988]. The four sites in a
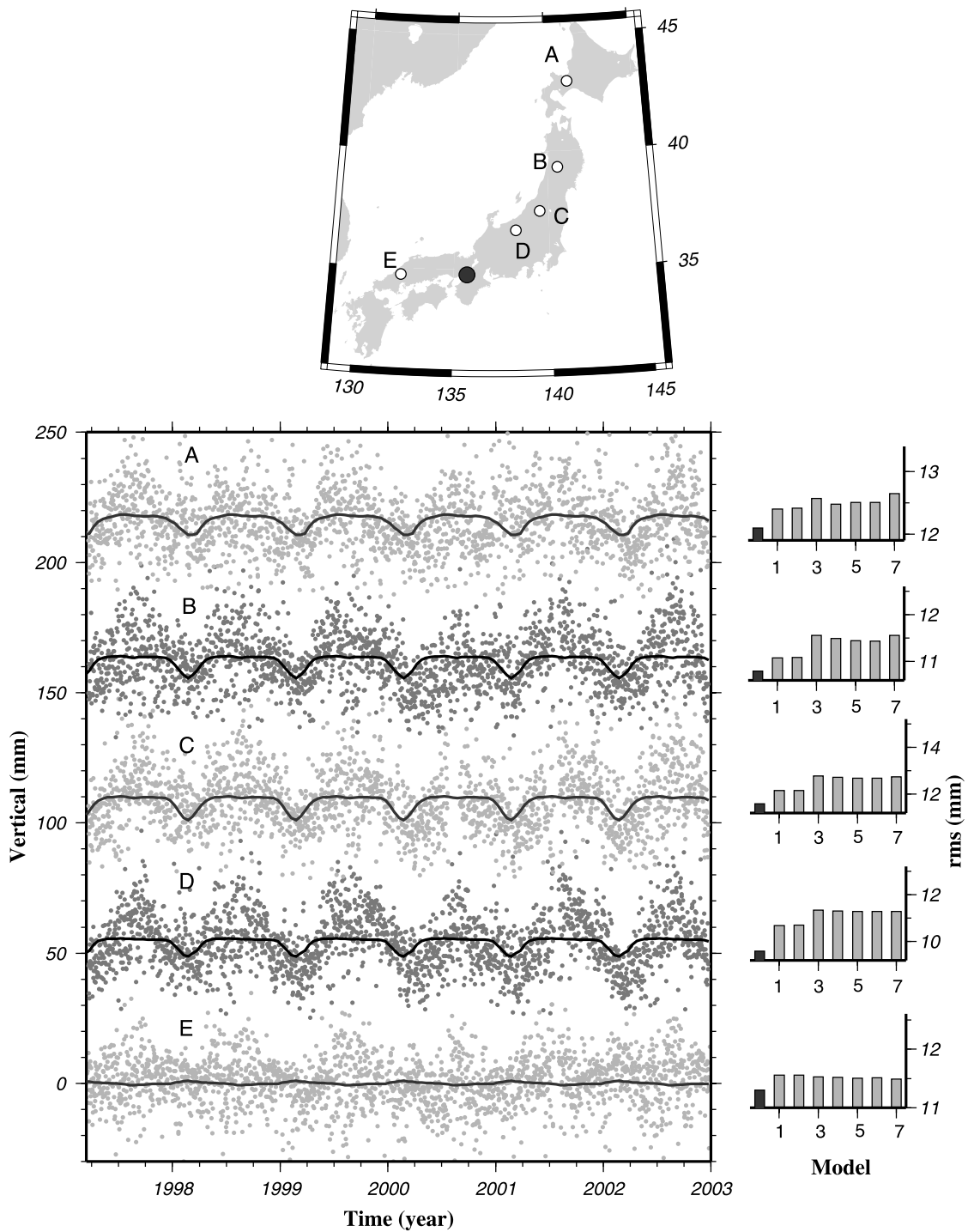
**Figure 16.** Seasonal change in vertical positions for five GPS stations (white circles in the map at the top) relative to a reference station (black circle in the map). Dots are GPS daily solutions in which secular components are removed (A,C,E and B,D are shown with different darkness for visual clarity). Curves denote synthesized seasonal variations. See the caption of Figure 14 for detail.
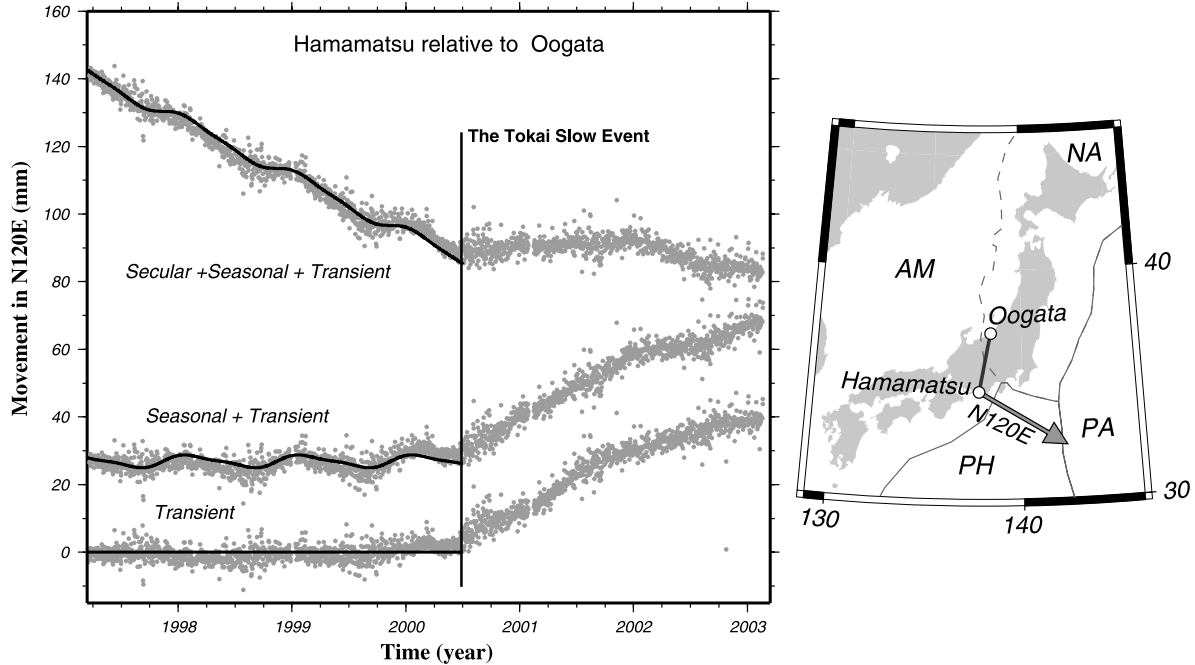
**Figure 17.** Movement in the ESE direction of the Hamamatsu GPS station, in the Tokai area, with respect to the Oogata station (see the map to the right for locations). The raw data (left, up) includes secular, transient, and seasonal components. The left middle curve is de-trended, and in the left lower curve seasonal changes are also removed. Seasonal and secular movements are inferred using the time series before the onset of the 2000 Tokai Slow Event [*Ozawa et al.*, 2002]. Solid curves indicate modeled secular and seasonal components. Abbreviations in the map denote tectonic plates, i.e. the North American (NA), Pacific (PA), Amurian (AM) and Philippine Sea (PH).

snowy area in Figure 16 are at much higher elevations than the fixed reference. Large height difference, i.e. large contribution of tropospheric delay to the site-to-site phase differences, makes the estimated vertical coordinates more susceptible to systematic errors. In addition to the height difference, existence of large atmospheric delay gradients in summer may have increased the vertical coordinate errors [*Iwabuchi et al.,* 2003; *Miyazaki et al*., 2003].

## 4. DISCUSSION

### 4.1. Interannual Changes and Isolation of Transient Signals

The depths of snow cover, the largest seasonally changing load in Japan, vary from year to year by tens of percents. The AMeDAS record (Plate 1) indicates that the snow depths were relatively small during the three winters from the end of 1996 to the early 1999, and has been relatively large for the next three winters. Such tendency might be present in amplitudes of wintry negative peaks in Figures 14–16 but its significance seems marginal. Change in amplitudes of annual signals in GPS data is reported by *Yamamoto* [2003]; he suggested that the amplitudes increased at the beginning of 2000.

*Kedar et al.* [2003] discussed the effect of second order ionospheric delay, which is not considered yet by standard GPS data analysis software packages, on GPS positioning. The 11 years solar activity period has been increasing the Total Electron Content (TEC) during the time period shown in Figures 14–16. This might be related to the increasing amplitudes of seasonal signals.

As mentioned before, investigation of seasonal signals is important to isolate transient crustal deformation signals out of the mixture of secular, transient and periodic crustal movements. Figure 17 shows the time series of east–southeastward component of the Hamamatsu station coordinate relative to Oogata. Hamamatsu is just above the focal region of the ongoing Tokai slow event [*Ozawa et al.,* 2002], and Oogata is fairly much affected by seasonal crustal movement due to snow load. They result in complicated time series made up of multiple components. Sudden departure in the middle of 2000 from the normal trend corresponds to the onset of the Tokai event. Such a transient signal is better perceived by removing secular components (Figure 17 left, middle), or both secular and seasonal components (Figure 17 left, below).

The "isolated" transient signal seems to indicate that the slow fault slip decelerated sometime in 2001 autumn as rec-

ognized by a small break of the curve. There I modeled the secular and seasonal components (in this case, annual plus semiannual) empirically using the three-year time series before the start of this event. Such an extrapolation is based on the implicit expectation that seasonal variations behave similarly every year. As suggested by the snow load variation shown in Figure 2, this may not be the case, and the slowing down of the Tokai transient signal in Figure 17 might only reflect inappropriate removal of seasonal signals. Slow fault slips in transient depths of subduction zones are often associated with non-volcanic tremor activities [*Rogers and Dragert,* 2003]. Such tremor activities are also present in the Tokai area [*Obara*, 2002], and their temporal changes may provide independent information on the change in the slow slip rate. At the moment, the seasonal coordinate change models are not sufficiently accurate (especially vertical components in summer, behaviors of interannual variations). The ultimate goal of the future seasonal crustal deformation studies is to make it possible to perform a-priori correction of seasonal signals in near real time, e.g. by using the current snow depth, and other loading data inferred by meteorological sensors and geophysical models.

## 4.2. Load Changes and Triggering of Inland Earthquakes

Seismic activity in some regions in Japan is known to change seasonally as mentioned in the introduction. Using the newest earthquake catalog, *Heki* [2003] recognized the tendency that inland earthquakes in snow-covered regions in Japan occur more in spring and summer as originally suggested by *Okada* [1982], and concluded that it may be related to the removal of snow load. In the present study, other kinds of loads have been evaluated (Figures 5–8), and the snow was found to be by far the largest seasonally changing load in Japan. This thus justifies the approach by *Heki* [2003]. Interplate thrust event along the Nankai, Suruga and Sagami Troughs are known to occur mainly in autumn and winter [*Ohtake and Nakahara*, 1999]. This is qualitatively consistent with the seasonal change of non-tidal oceanic loads; the SSH shows maximum in August and September (Figure 9), and the highest seismicity in December coincide with the period of the rapid load removal (this period comes 1/4 year after the SSH peak). However, thermal steric correction may be still imperfect, and the deployment of ocean bottom pressure gauges around Japan to monitor in-situ water mass changes above the sensor [e.g. *Fujimoto et al.*, 2003] would derive final conclusion for their causal relationship.

It is meaningful, in seismically active parts of the world, to understand the relative importance of all possible sources of seasonal loads, and evaluate their influences upon seismicity. *Gao et al.* [2000] considered the seasonal atmospheric pressure

changes with peak-to-peak amplitudes of about 2 kPa as the main cause of seasonal modulation of seismicity in California. On the other hand, *Saar and Manga* [2003] attributed the seasonal change in seismicity in Oregon, USA to the pore pressure changes associated with the change in precipitation. Similar discussion is also done world-wide by *Matsumura* [1986]. The method described here to evaluate various seasonally changing loads would be applicable for such studies.

## 5. CONCLUDING REMARKS

I performed comprehensive studies of changing loads within the Japanese Islands, i.e. snow, atmosphere, soil moisture, water impoundment of reservoirs, and over the oceanic area around Japan, and calculated crustal deformation caused by them. Then synthesized seasonal coordinate change signals are compared with real data observed by the dense GPS array. The following conclusions have been obtained,

(1) In Japan, by far the largest contribution comes from snow, and it causes a few mm arc-normal contractions and subsidence of up to 1 cm in northeastern Japan in winter. To evaluate snow contributions quantitatively, special attentions are needed for the altitude correction of the snow depth data, and for temporal changes of average snow densities.

(2) Other loads are of minor importance in Japan, being atmosphere the second largest source to snow. However, the order of importance would change in other parts of the world.

(3) Seasonal change in scales of unknown origin exists in the GEONET solution.

(4) Seasonal change in atmospheric gradients also contributes to seasonal signals in some areas [*Hatanaka*, 2003a], and it is preferable to estimate gradient parameters in the GEONET official solutions in the future.

(5) Amplitudes and waveforms predicted by the changing loads and scales are mostly in accordance with real GEONET data, although small inconsistency remains in summer behaviors.

(6) Understanding of seasonal signals including their interannual changes is important to isolate transient crustal deformation signals.

(7) Seasonal change in the occurrences of inland earthquakes is possibly influenced by snow loads. Seasonality in submarine interplate earthquakes needs further investigation.

Study of mass redistribution is one of the main targets of recent satellite gravity missions, e.g. CHAMP and GRACE [*Reigber*, 2003]. However, those in relatively small spatial scales, as studied in the Japanese Islands here, are still too small to be detected with their current accuracy. From this point of view, dense GPS arrays would play a complementary role to these satellite missions by detecting surface mass changes with relatively short wavelength and large amplitudes.

# REFERENCES

Altamimi, Z., P. Sillard, and C. Boucher, ITRF2000: A new release of the International Terrestrial Reference Frame for earth science applications, *J. of Geophys. Res.,* 107, 2214, doi:10.1029/2001JB000561, 2002.

Beutler, G., I. Bauersima, W. Gurtner, M. Rothacher, T. Schildknecht, and A. Geiger, Atmospheric refraction and other important biases in GPS carrier phase observations, *Monograph 12*, School of Surveying, Univ. New South Wales, Kensington, pp.26, 1988.

Blewitt, G., D. Lavallée, P. Clarke, and K. Nurutdinov, A new global mode of earth deformation: seasonal cycle detected, *Science,* 294, 2342–2345, 2001.

Bouille, F., A. Cazenave, J. M. Lemoine, and J.F. Crétaux, Geocenter motion from the DORIS space system and laser data on Lageos satellites: Comparison with surface loading data, *Geophys. J. Int.,* 143, 71–82, 2000.

Cazenave, A., Global-scale interactions between the solid earth and its fluid envelopes at the seasonal time scale, *Earth Planet. Sci. Lett.,* 171, 549–559, 1999.

Chao, B.F., Anthropogenic impact on global geodynamics due to reservoir water impoundment, *Geophys. Res. Lett,* 22., 3529–3532, 1995.

Chao, B.F., and A.Y. Au, Atmospheric excitation of the Earth's annual wobble, 1980–1988, *J. of Geophys. Res.,* 96, 6577–6582, 1991.

Crétaux, J.-F., L. Soudarin, F.J.M. Davidson, M.-C. Gennero, M.Bergé-Nguyen, and A. Cazenave, Seasonal and interannual geocenter motion from SLR and DORIS measurements: Comparison with surface loading data, *J. of Geophys. Res.,* 107, 2374, doi:10.1029/2002JB001820, 2002.

Dong, D., J.O. Dickey, Y. Chao, and M.K. Cheng, Geocenter variations caused by atmosphere, ocean and surface ground water, *Geophys. Res. Lett.,* 24, 1867–1870, 1997.

Dong, D., P. Fang, Y. Bock, M.K. Cheng, and S. Miyazaki, Anatomy of apparent seasonal variations from GPS-derived site position time series, *J. of Geophys. Res.,* 107, 10.1029/2001JB000573, 2002.

Farrell, W.E., Deformation of the Earth by surface loads, *Rev. Geophys. Space Phys.,* 10, 761–797, 1972.

Fujimoto, H., M. Mochizuki, K. Mitsuzawa, T. Tamaki, and T. Sato, Ocean bottom pressure variations in the southeastern Pacific following the 1997–98 El Niño event, *Geophys. Res. Lett.,* 30, 1456, doi:10.1029/2002GL016677, 2003.

Gao, S.S., P.G. Silver, A.T. Linde, and I.S. Sacks, Annual modulation of triggered seismicity following the 1992 Landers earthquake in California, *Nature,* 406, 500–504, 2000.

Hachikubo, A., T. Kaihara, and Y. Ito, Report of pit-wall observations of snow cover in Sapporo 1996–97, *Low Temperature Sci., Ser. A., Data Report,* 56, 1–8, 1997 (in Japanese with English abstract).

Hatanaka, Y., A. Sengoku, T. Sato, J.M. Johnson, C. Rocken, and C. Meertens, Detection of tidal loading signals from GPS permanent array of GSI Japan, *J. of Geod. Soc. Japan,* 47, 187–192, 2001.

Hatanaka, Y., Seasonal variation of scale of GEONET network and ZTD biases, *paper presented at the Symposium JSG01,23rd IUGG General Assembly, Sapporo, Japan,* July 7, 2003a.

Hatanaka, Y., Improvement of the analysis strategy of GEONET, *Bull. of Geograph. Survey Inst.,* 49, 11–37, 2003b.

Heki, K., Seasonal modulation of interseismic strain buildup in Northeastern Japan driven by snow loads, *Science,* 293, 89–92, 2001.

Heki, K., Snow load and seasonal variation of earthquake occurrence in Japan, *Earth Planet. Sci. Lett.,* 207, 159–164, 2003.

Heki, K., S. Miyazaki, and H. Tsuji, Silent fault slip following an interplate thrust earthquake at the Japan Trench, *Nature,* 386, 595–598, 1997.

Hirose, H., K. Hirahara, F. Kimata, N. Fujii, and S. Miyazaki. A slow thrust slip event following the two 1996 Hyuganada earthquakes beneath the Bungo Channel, Southwest Japan, *Geophys. Res. Lett.,* 26, 3237–3240. 1999.

Hugentobler, U., S. Schaer, and P. Fridez (eds.), *Bernese GPS Software Version 4.2*, Astronomical Institute, University of Berne, pp 515, Bern, 2001.

Iwabuchi, T., S. Miyazaki, K. Heki, I. Naito and Y. Hatanaka, An impact of estimating tropospheric delay gradients on tropospheric delay estimations in the summer using the Japanese nationwide GPS array, *J. of Geophys. Res.,* 108, 4315, doi:10.1029/2002JD002214, 2003.

Kato, T., Secular and earthquake-related vertical crustal movements in Japan as deduced from tidal records (1951–1981), *Tectonophys.,* 97, 183–200, 1983.

Kazama, S., and M. Sawamoto, Estimation of the snow depth distribution and water resources volume using NOAA/AVHRR, *J. Japan Soc. Hydrol. Water Resour.,* 8, 477–483, 1995 (in Japanese with English abstracts).

Kedar, S., G.A. Hajj, B.D. Wilson, and M.B. Heflin, The effect of the second order GPS ionospheric correction on receiver positions, *Geophys. Res. Lett.,* 30, 1829, doi:10.1029/2003GL017639, 2003.

MacMillan, D.S., Atmospheric gradients from very long baseline interferometry observations, *Geophys. Res. Lett.,* 22, 1041–1044, 1995.

Matsumura, K., On regional characteristics of seasonal variation of shallow earthquake activities in the world, *Bull. of Disas. Prev. Res. Inst., Kyoto Univ.,* 36, 43–98, 1986.

McCarthy, D.D. (Ed.), IERS Conventions 1996, *IERS Tech. Note 21*, Int. Earth Rotation Serv., Obs. de Paris, Paris, Jul. 1996.

Milly, P.C.D., Climate, soil water storage, and the average annual water balance, *Water Resour. Res.,*30, 2143–2156, 1994.

Miyazaki, S., T. Iwabuchi, K. Heki, and I. Naito, An impact of estimating tropospheric gradient on precise positioning in summer using the Japanese nationwide GPS array, *J. of Geophys. Res.,*

108, 2335, doi:10.1029/2000JB000113, 2003.

Munekane, H., M. Tobita, K. Takashima, S. Matsuzaka, Y. Kuroishi, and Y. Masaki, Groundwater-driven vertical movement in Tsukuba detected by GPS, *paper presented at the American Geophys. Union, 2003 Fall Meeting*, San Francisco, USA, Dec. 12, 2003.

Munk, W.H., and G.J.F. MacDonald, *The Rotation of the Earth, a Geophysical Discussion*, Cambridge University Press, 323pp, 1960.

Murakami, M., and S. Miyazaki, Periodicity of strain accumulation detected by permanent GPS array: possible relationship to seasonality of major earthquakes' occurrence, *Geophys. Res. Lett.,* 28, 2983–2986, 2001.

National Astronomical Observatory (ed.), *Chronological Scientific Tables,* 76, 942pp, Maruzen, 2002..

National Res. Inst. For Earth Sci. Disaster Prevention (NIED), Interesting phenomena detected by Sakata-type three-component strainmeters, *Rept. Coord. Comm. Earthq. Pred.,* 69, 205–211, 2003 (in Japanese)

Obara, K., Nonvolcanic deep tremor associated with subduction in southwest Japan, *Science,* 296, 1579–1681, 2002.

Ohtake, M., and H. Nakahara, Seasonality of great earthquake occurrence at the northwestern margin of the Philippine Sea Plate, *Pure Appl. Geophys.,* 155, 689–700, 1999

Okada, M., Seasonal variation in the occurrence rate of large earthquakes in and near Japan and its regional differences, *Zisin* 2, 35, 53–64, 1982 (in Japanese with English abstracts).

Ozawa, S., M. Murakami, M. Kaidzu, T. Tada, T. Sagiya, Y. Hatanaka, H. Yarai, and T. Nishimura, Detection and monitoring of ongoing aseismic slip in the Tokai Region, Central Japan, *Science,* 298, 1009–1012, 2002.

Ozawa, S, S. Miyazaki, Y. Hatanaka, T. Imakiire, M. Kaidzu, and M. Murakami, Characteristic silent earthquakes in the eastern part of the Boso Peninsula, Central Japan, *Geophys. Res. Lett.,* 30, doi: 2002GL016665, 2003.

Reigber, C., The gravity field of the Earth determined by new satellite missions, *paper presented at the Symposium U6,23rd IUGG General Assembly,* Sapporo, Japan, July 9,2003.

Rogers, G. and H. Dragert, Episodic tremor and slip on the Cascadia subduction zone: the chatter of silent slip, *Science,* 300, 1942–1943, 2003.

Saar, M.O., and M. Manga, Seismicity induced by season groundwater recharge at Mt. Hood, Oregon, *Earth Planet. Sci. Lett.*, 214, 605–618, 2003.

Sato, T., Y. Fukuda, Y. Aoyama, H. McQueen, K. Shibuya, Y. Tamura, K. Asari, and M. Ooe, On the observed annual gravity variation and the effect of sea surface height variations, *Phys. Earth Planet. Inter.,* 123, 45–63, 2001.

Stammer, D., R. Tokmakian, A. Semter, and C. Wunsh, How well does a 1/4° global circulation model simulate large-scale oceanic observations? *J. of Geophys. Res.,* 101, 25779–25811, 1996.

Thornthwaite, C.W., An approach toward a rational classification of climate, *Geogr. Rev.,* 38, 55–94, 1948.

van Dam, T.M., G. Blewitt, and M. Heflin, Detection of atmospheric pressure loading using the Global Positioning System, *J. of Geophys. Res.* 99, 23,939–23,950, 1994.

van Dam, T.M., J. Wahr, P.C.D. Milly, A.B. Shmakin, G. Blewitt, D. Lavallée, and K. M. Larson, Detection of atmospheric pressure loading using the Global Positioning System, *Geophys. Res. Lett.,* 28, 651–654, 2001.

Wahr, J.M., M. Molenaar, and F. Bryan, Time variability of the Earth's gravity field: Hydrological and oceanic effects and their possible detection using GRACE, *J. of Geophys. Res.,* 103, 30,205–30,229, 1998.

Wang, H., H.T. Hsu, and Y.Z. Zhu, Prediction of surface horizontal displacements, and gravity and tilt changes caused by filling the Three Gorges Reservoir, *J. of Geodesy,* 76, 105–114, 2002.

Wu, X.-P., M.B. Heflin, E.R. Ivins, D.F. Argus, and F.H. Webb, Large-scale global surface mass variations inferred from GPS measurements of load-induced deformation, *Geophys. Res. Lett.,* 30, 1742, doi:10.1029/2003GL017546, 2003.

Yamamoto, T., Change in the annual variation patterns of the GEONET site coordinate time series and its implication for the analysis of the Tokai Slow Event, *The Earth Monthly*, 41, 71–76, 2003 (in Japanese).

Yamaya, M., K. Numazawa, K. Yano, A. Kumagai, H. Abiko, A. Sato, H. Abe, Observation of icing and snow accretion on Jyuhyo (Ice Monsters) at Mt.Zao, *Tohoku J. Natural Disaster Sci.,* 36, 171–176, 2000 (in Japanese).

Kosuke Heki, Division of Earth Rotation, National Astronomical Observatory, 2–12 Hoshigaoka, Mizusawa, Iwate 023–0861, Japan. (heki@miz.nao.ac.jp).